A study of a single droplet impinging onto a sloped surface: Jet-Fuel and Biofuel mixtures

Inês Ferrão[1], Jorge Barata[1] and André Silva*[1]
[1]AEROG – LAETA, University of Beira Interior, Covilhã, Portugal
Corresponding author: andre@ubi.pt

Abstract
The present study experimentally investigated droplets impinging on a sloped aluminum surface. In these experiments, the droplet is spherical throughout the trajectory where the gravitational acceleration and movement of the droplet have the same direction, which leads to unique phenomena. Considering an oblique impact, the droplet collides with a certain angle, and the impact velocity is composed of normal and tangential components to the surface that vary with the impact height. Four fluids were tested: 100% Jet-Fuel, 75% Jet-Fuel/ 25% HVO, 50% Jet-Fuel/ 50% HVO and H_2O (pure water) as a reference. The mixtures were a combination of a conventional Jet Fuel (Jet A-1) and a biofuel (HVO – Hydroprocessed Vegetable Oil), more specifically NExBTL. When a droplet impacts onto an inclined surface, its shape is distorted and it can spread or splash asymmetrically relatively to the point of impact, affecting the advancing and receding contact angle. Therefore, several geometric parameters were measured and compared for the different fluids and incident angles. The incident angles influence the spreading velocity on the upper and lower side. The spreading velocity was analyzed, allowing a better understanding of the dynamic behavior of each side. The spread factor, which corresponds to the distance between the lower and upper edges normalized by the initial droplet diameter, was compared to the Weber number (*We*) which is a proper indicator for the drop deformation. The variation of incident angles and impact velocity promotes a different droplet movement and asymmetry in phenomena that are also evidently influenced by the gravity role.

Keywords: Droplet impingement, Oblique impact, Jet-Fuel and Biofuel

---

Introduction

Over the years, science and technological development had significant progress and profound influence on the scientific community. Several studies were performed due to the fascination and interest in reaching a better understanding of droplet - wall interaction. The knowledge of droplet impingement is relevant for a wide variety of applications, such as fuel injection in internal combustion engines, processes involving spray coating, spray paints and cooling of electronic equipment. The desired phenomenon varies according to the application. There are many factors that influence the outcome: impact velocity, droplet morphology, fluid properties, surrounding environment, among others. The impact on dry surfaces is conditioned by the surface characteristics such as wettability and roughness [1]. Wettability describes the ability of a liquid to spread on a solid and can be represented by the angle between the contour of the droplet surface and the interface liquid/solid. This angle is denominated by the static contact angle (θ_{static}) and is measured when the droplet stays static on the surface. The contact angle decreases when the wettability increases. High wettability corresponds to small contact angles ($\theta_{static} < 90º$), while low wettability corresponds to large contact angles ($\theta_{static} > 90º$). However, when the three-phase boundary (solid-liquid-gas) are moving, the dynamic contact can be measured, which can be denominated as advancing and receding angles. The advancing contact angle (θ_a) is always larger than or equal to the receding contact angle (θ_r). The difference between these contact angles can be defined as contact angle hysteresis. For an inclined surface, the advancing and receding contact angle and droplet geometry were predicted to vary with surface inclination [2]. The droplet geometry is crucial to understand condensation and evaporation of liquid droplets from a surface, the rate of heat transfer through a droplet and the forces acting [3].
When a liquid droplet is placed on a sloped surface, it tends to flow downwards, partially wetting the surface. For a droplet impacting onto an inclined surface, an incident angle (α) appears and the impact velocity is composed of normal (u_n) and tangential (u_t) components (figure 1). According to Yao and Cai [5], if the incident angle (α) is not *90º*, the tangential velocity component acts to destabilize the spreading liquid film, hence, to enhance the fragmentation of the droplet following the impingement.
A few years later, Chen and Wang [6] studied the effects of the tangential speed on the collision outcome. In their experiments, for a higher We_n and a constant We_t, the latter had fewer effects on the collision and the duration from impact to retraction was shorter.

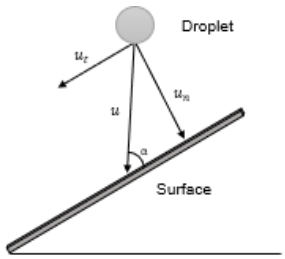

Figure 1. Illustration of incident angle (α) and impact velocity (u).

For an increase in We_t, the spreading of the droplet on the solid surface in the t-direction increased. To explain and understand the influence of tangential velocity component in the phenomena observed, Bird et al. [7] noticed that, based on the magnitude of this velocity component, there are three possible behavior: the lamella spreads in all directions, splash in all directions or asymmetrically splash. When there is no tangential velocity component, the droplets either spread or splash in all directions. Another factor with significant importance for the droplet deformation is the incident angle (α). Jayaratne and Mason [8] reported that the outcome depends largely on the incident angle, which also influences the direction of the secondary droplets for smooth surfaces. Additionally, Liu et al. [9] studied the effects of droplet velocity, impact angle and ambient pressure on the splashing threshold. They performed experimental investigations of splashing varying the incident angle and concluded that to reduce splash and increase the spreading velocity, a decrease in the incident angle is required. The magnitude of splashing it is also influence by the Weber number. This assumption was also discussed by Yeong et al. [10] and Liang et al. [11] which reported that an increase of We promotes splashing. Recently, Hao et al. [12] performed a study using an inclined surface and found that the velocity of the lamella tip determines the splash onset. Thus, the existing splash can be asymmetric for the different incident angles. When a droplet impacts onto a sloped surface, the splash can occur on the lower, upper or both sides. According to Zen et al. [13], a hypothesis for the asymmetric splash is the component of gravity parallel with the inclined surface. This component promotes an opposite influence on the lower and upper sides in the spreading stage. The incident angle also affects the formation of secondary droplets. Several authors, J.Bikerman [14], Liang et al. [15], Shen et al. [16] and Šikalo et al. [17], studied the influence of the incident angle on the development and motion of the droplet after impinging onto an inclined surface. It was pointed out by J. Bikerman [14] that, when a droplet is placed on a plate, its base is approximately circular. However, if the plate is slowly tilted, the droplet becomes elongated in the direction of the inclination. The elongation of the droplet is related to an asymmetric deformation and sliding motion, dominated by the gravity effect. The sliding occurs when the inclination angle reaches a critical value beyond a component of the droplet weight that can no longer be supported by the surface tension [2]. To evaluate the dynamic behavior of a droplet after impacting on a sloped surface, the spread factor can be considered, which corresponds to the distance between the edges normalized by the initial droplet diameter. Šikalo et al. [17] observed that for lower incident angles lead to a larger droplet elongation and the spreading in the upper side is less due to the small inertial forces associated with the low normal velocity. Although the smaller normal velocity component, the lamella remains to be developed along the inclined surface due to the increased parallel velocity component [18]. In the initial phase the inertial forces dominate and, in the later stages, gravity becomes more significant. According to Basit et al. [19], wettability is not relevant in the first stage of spreading when the impact velocity is high because the droplet is spreading under inertia. Wettability only has influence when the lamella has slow velocity. A brief discussion of various works shows that not only the variation incident angle has a huge relevance on the impact of droplets onto the sloped surface but also the Weber number. Cui et al. [20] developed an experimental study with the purpose of analyses the droplet morphology after impact for different incident angles and Weber numbers. They concluded that the maximum spread diameter increases with the Weber number when the incident angle is constant, and the droplet starts to recoil when it reaches the maximum spreading diameter. The increase of the impact velocity promotes a faster spreading whereas an increase of surface tension and viscosity contributes to a slower spreading [21]. Liang et al. [22] described the effect of the physical properties of fluids and incident angle on spreading and splashing of a single droplet impinging on an inclined wetted surface. In their work was reported that the initiatory spread velocity can be increased by increasing the impact velocity and incident angle, which are influenced by the pre-existing film thickness and the tangential component of the impact velocity. The tangential velocity is crucial for the spreading on the lower side, whereas for the upper side it means a resistance. Therefore, the difference in the spread velocity of the lamellas in the lower and upper side increases with a decrease of incident angle, as reported by Šikalo et al. [17]. In the present work, we discuss the dynamic behavior of a single droplet impinging on an inclined surface. Herein, we provided the influence of the incident angle and impact velocities on the droplet morphology subsequent to impact, spread factor and spread velocity.

Experimental Approach

Figure 2 shows a schematic of the experimental facility used in the present work. The experimental system consists of four main components: image acquisition, droplet dispensing system, impact surface, and illumination. For the image acquisition, a high-speed camera Photron FASTCAM mini UX50 with 1.3 Megapixel was used. This high-speed camera was connected to a computer and manually triggered to facilitate the image procurement. A Macro Lens Tokina AT-X M100 AF PRO D with a minimum focus distance of *300mm*, a focal length of *100mm*, a macro ratio of 1:1 and a filter size of *55mm*, was also used. To allow the visualization of the droplet deformation, two different views of the phenomenon was performed. For the side view, the image acquisition was pursued with *5000fps* (frames per second), leading to a resolution of 1280x488 pixels. Regarding the front view, *2500fps* and *3200fps* were considered, which correspond to an image resolution of 1280x800 and 1280x720 pixels, respectively. The droplet dispensing includes a needle with an inner diameter of *1.5mm* that is connected to a syringe with a volume of *50ml* and a syringe pump which allows a pumping rate of *0.5ml/min*. The droplets generated leave the straight tip of the needle when the gravity exceeds the force due to surface tension. The impact velocity was changed when the distance between the impact surface and the needle was varied. For the impact surface, an apparatus was designed and elaborated that has the possibility to vary the incident angles from *10º* to *90º*. This mechanism has a smooth, dry aluminum plate with a mean roughness of *0.13µm*. To intensify the contrast and to improve the phenomena visualization, the room was completely dark, and the illumination was parallel to the falling plane. To provide uniform illumination, a diffusion glass was placed between the lighting and the impact surface.

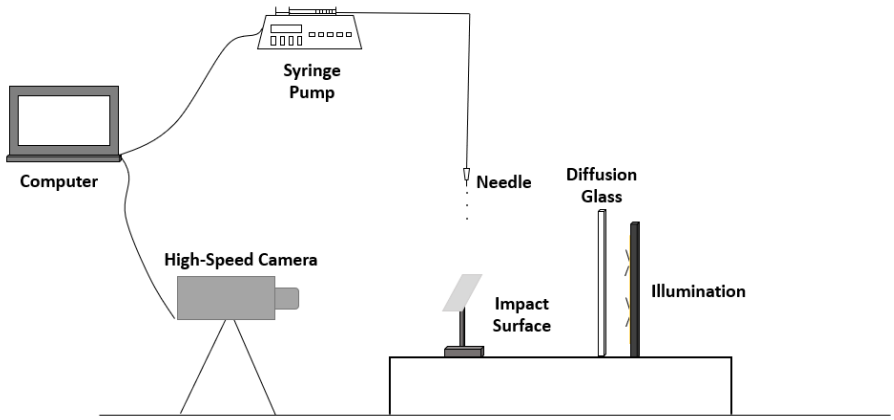

Figure 2. Schematic of the experimental facility.

For the characterization of the droplets, image data processing was performed. To determine the impact velocity, droplet diameter, and the geometric parameters after impact, the MATLAB software was used. Firstly, an algorithm was developed in order to subtract and binarize the images with the purpose of determining the number of pixels correspondent to the droplet diameter, width and length of the spreading. For the impact velocity, a function was used to determine the droplet centroid. For this analysis, three frames were considered, which included a background frame and two frames with the droplet distancing *1.4ms* before impact. This was only possible through image binarization and pixel size values.

Table 1 summarizes the physical properties of the four fluids used in the present work. The density (ρ), surface tension (σ) and viscosity (μ) for the 100% Jet-Fuel, 75%JF-25%HVO, 50%JF-50%HVO were measured. The values for density and surface tension are approximately identical and the major difference is the viscosity. The mixtures were chosen taking in consideration that the civil aviation regulation only allows blends with at least 50% Jet-Fuel in volume. The density was determined with the pycnometer method and the error is ±0.01g. For the surface tension, the equipment used was the Data Physics using the pendant droplet method with an accuracy of 0.6%. To measure the fluids viscosities, it was used a Brookfield DV3TRVCP Rheometer and the accuracy is ± 1.0% [23].

Table 1. Physical properties and diameter of the fluids.

	100%JF	75%JF-25%HVO	50%JF-50%HVO	H_2O
ρ [kg m^{-3}]	798	795	792	1000
σ [mN m^{-1}]	25.4	25.5	24.6	72.8
μ [mPa.s]	1.12	1.44	1.79	1.0
D_0 [mm]	3.0	3.1	3.1	4.1

Results and discussion

Droplet morphology

The behavior of a droplet when impacting onto an inclined surface is quite different from a droplet colliding perpendicularly to a surface. In this section, we will present the influence of the incident angle and impact velocity on the droplet deformation. Figure 3 shows a sequence of images correspondent to a 50%JF-50%HVO droplet impinging onto a sloped surface with three different incident angles and a similar impact velocity of approximately u*=4m/s*. For the three incident angles, splashing was the phenomenon observed. Splashing is characterized by the formation of secondary droplets due to a high impact energy when the droplet collides onto a dry or wetted surface. In figure 3, each column represents a different incident angle for *We=1600*. When a 50%JF-50%HVO droplet impinges upon a dry inclined surface with an incident angle of $\alpha = 75^{o}$, the splash occurs evidently on the upper and lower side. In the lower side, a crown splashing is developed and a few, small secondary droplets are ejected from the upper side, corresponding to an asymmetric splash. For $\alpha = 45^{o}$, splash on the upper side is suppressed. Regarding the lower side, the splash is weaker when compared to $\alpha = 60^{o}$ and $\alpha = 75^{o}$. The same analogy was performed for $\alpha = 60^{o}$. Thus, splash decreases with the decrease of the incident angle, as displayed in figure 3.

For the impact onto an inclined surface, the gravity has an influence on the outcome. Zen et al. [13] reported that the tangential component of gravity promotes an opposite contribute for the upper and lower side. This is a possible reason for the suppression of splash in the upper side.

The different rows represent different stages after impact. In the early stages, several secondary droplets are observed, and then the development of the crown became more perceptible, as can be seen in t = 0.6ms.

These results show that the droplet deformation is influenced by the variation of incident angles, as reported by Liu et al. [9], where the decrease of incident angles leads to a decrease of the splashing phenomena.

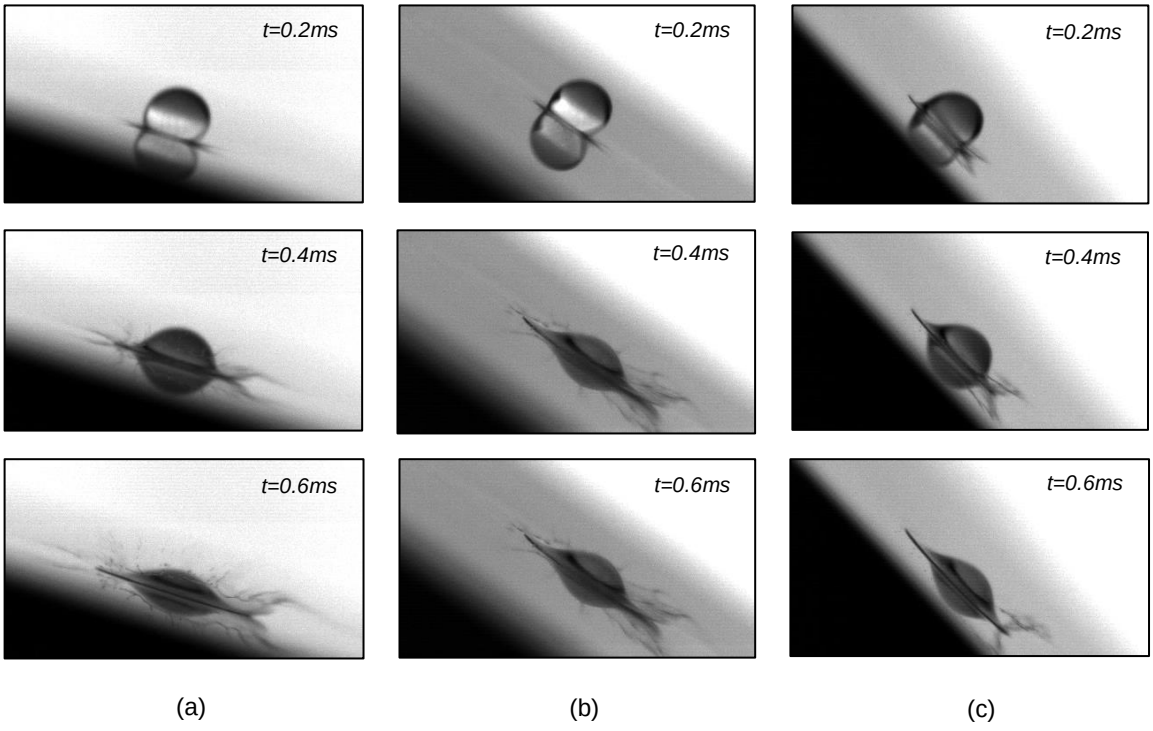

Figure 3. Sequence of images of 50%JF-50%HVO droplet (D_o*= 3.1mm,* u *= 4m/s, We=1600*); (a) $\alpha = 75^{o}$, (b) $\alpha = 60^{o}$; (c) $\alpha = 45^{o}$.

Figure 4 shows a comparison of an H_2O droplet impinging onto a dry inclined surface with an incident angle of $\alpha = 45^{o}$ for two different Weber numbers. This sequence of images is relevant to understand the influence of Weber numbers on the dynamic behavior of a droplet impacting on an inclined surface. For each Weber number, different views were acquired for a better visualization of the phenomenon. From the side view, in figure 4 (b), when *We=1080*, splash is spotted, and several secondary droplets are ejected from the lower side. However, when the Weber number decreases, splash does not occur, as can be seen in figure 4 (d). The effect of the Weber number affects not only the outcome but also the development of the droplet after impact. From the front view, there are significant differences on the droplet for the two Weber numbers.

In the later stages, when the Weber number is increased, fingering appears. Fingering occurs when instabilities are detected in the outer rim of the lamella at the beginning of the spreading phase, which can break-up in the last stages. This outcome is clearly visible for We=1080. At t =2.8ms, few finger structures are developed mainly on the lower side in the same direction as the growth of the lamella.

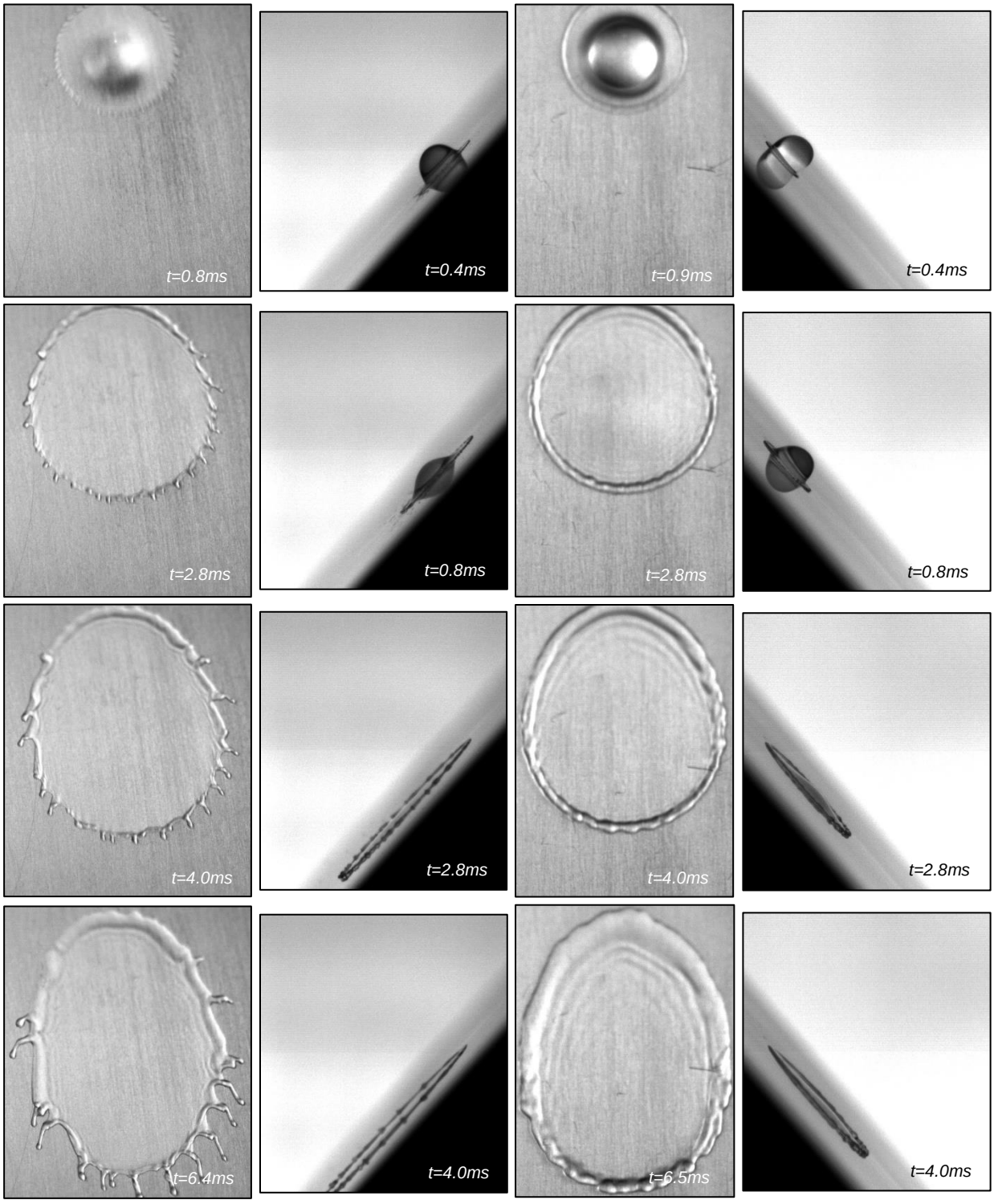

Figure 4. Sequences of images of H_2O droplet (D_0=*4.1mm*); (a) ***α = 45°***, *We=1080*, Front view, (b) ***α = 45°***, *We=1080*, Side view, (c) ***α = 45°***, *We=300*, Front view, (d) ***α = 45°***, *We=300*, Side view.

However, these finger structures, due to gravity, change the direction of the motion. Then, it begins to slide in the same direction as the inclination of the surface. As already mentioned, these fingers break up after growing ahead of the contact line and tiny droplets remain on the surface with an elliptical shape. This effect happens in the receding phase which occurs after the lamella reaches the maximum diameter. The influence of Weber number is evident on the spreading diameter. The difference in the transverse spreading diameter, for *We=1080* and *We=300,* is *6.9mm* and *3.9mm*, respectively. The spreading diameter is weaker with the development of the phenomenon.

Spread Factor

In general, the evolution of film after a droplet impinging onto a sloped surface is crucial to study several characteristics, which have relative importance for different applications. In the last years, the spread factor has been studied in an intensive way. The spread factor is defined as the distance between the edges normalized by the initial droplet diameter. Figure 5 exhibits the spread factor for each fluid used in this present work. Each graphic displays lines for three incident angles and two Weber numbers, and also takes into consideration the droplet slide. The spread factor is compared for the different fluids as a function of the dimensionless time ($\tau = tu/D_0$). The values of the expansion film have as reference the point of impact, and they are positive in the upward direction of the upper side and in the downward of the lower side. As already mentioned, in the early stages of spreading, the inertial forces dominate. When the incident angle is less than *90º*, the gravitational force acting on the liquid film will be weakened. This fact is perceptible due to the reduction of the normal component of the gravitational force which is influenced by the incident angle. At the beginning, for all the fluids, the spread factor increases with τ and then the evolution is quite different (figure 5). Lower incident angle (*α=45º*) shows that the development of the spread factor is smaller, which is generated by the decrease of the normal momentum. These conclusions were also observed by [17,18]. This observation was noticed for lower and higher Weber numbers.

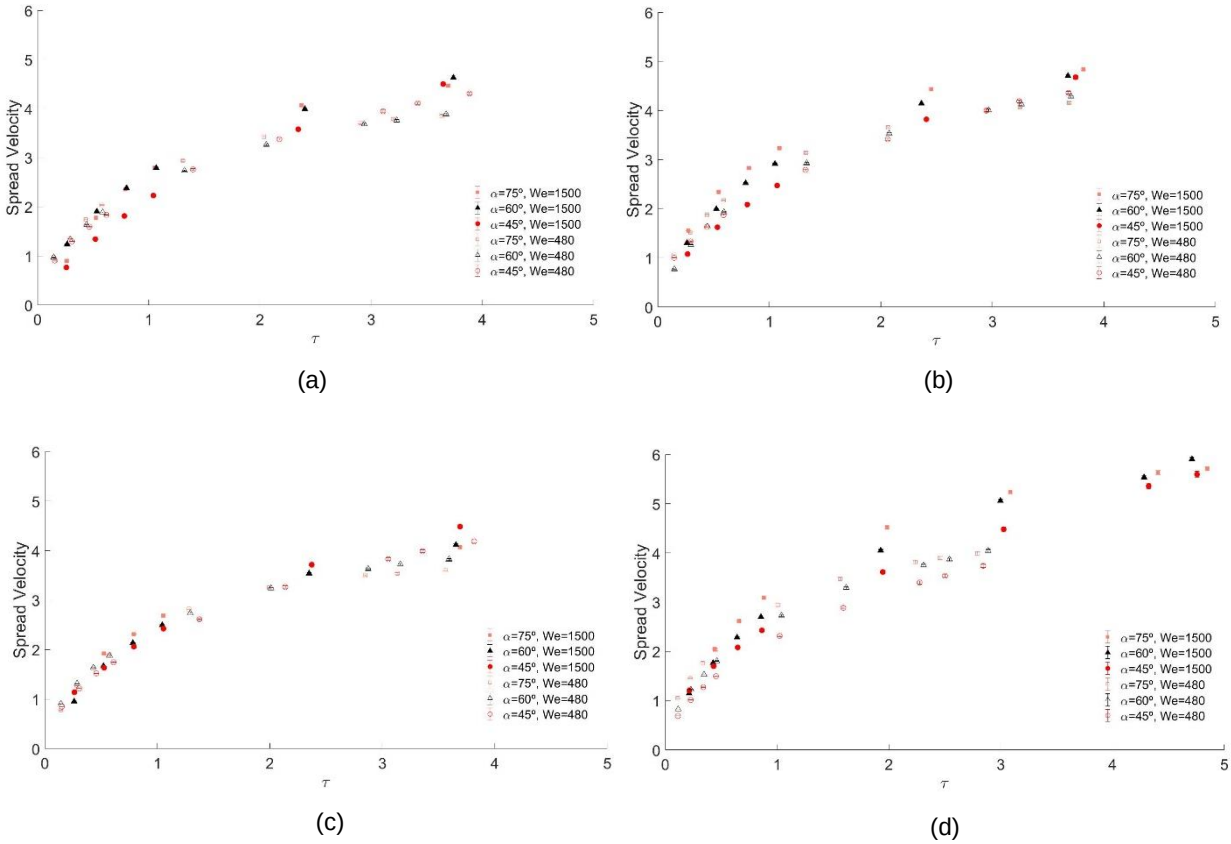

Figure 5. Spread factor as function of non-dimensional time; (a) 100% Jet-Fuel, (b) 75% Jet-Fuel – 25% HVO, (c) 50% Jet-Fuel – 50% HVO, (d) H_2O.

However, the dynamic behavior of the spreading starts to change for the interval between τ=3 and τ=4 and occurring later for H_2O. After that time, gravity begins to play a major role. Thus, the effect of gravity appears to promote the sliding of the liquid film, which is significantly evident for α = 45º. These results also demonstrate that the increase of the Weber number leads to an increase of the spread factor when the incident angle is constant.

Spread Velocity

Figure 6 presents the spread velocity normalized by the impact velocity. The spread velocity for 100%JF and 75% JF – 25% HVO was analyzed. Two different Weber numbers and three incident angles for the upper and lower side were compared. The spread velocity corresponds to the difference between the front length and back length of the expanding film with respect to impact time. Similarly, as the spread factor, the values of the expansion length of the film are positive taking into consideration the point of impact and the motion of the lamella. The results show that an increase of Weber number contributes to an increase in the spread velocity for a constant incident angle. On the other hand, a decrease of the incident angle leads to a higher difference in the spread velocity of the lamella on the lower and upper side. The spreading on the upper side is smaller than the lower side due to the small inertial forces correspondent to the normal component, as referenced by [17] . It is visible that the spread velocity in the lower side is larger than the upper side for both Weber numbers and all the incident angles.

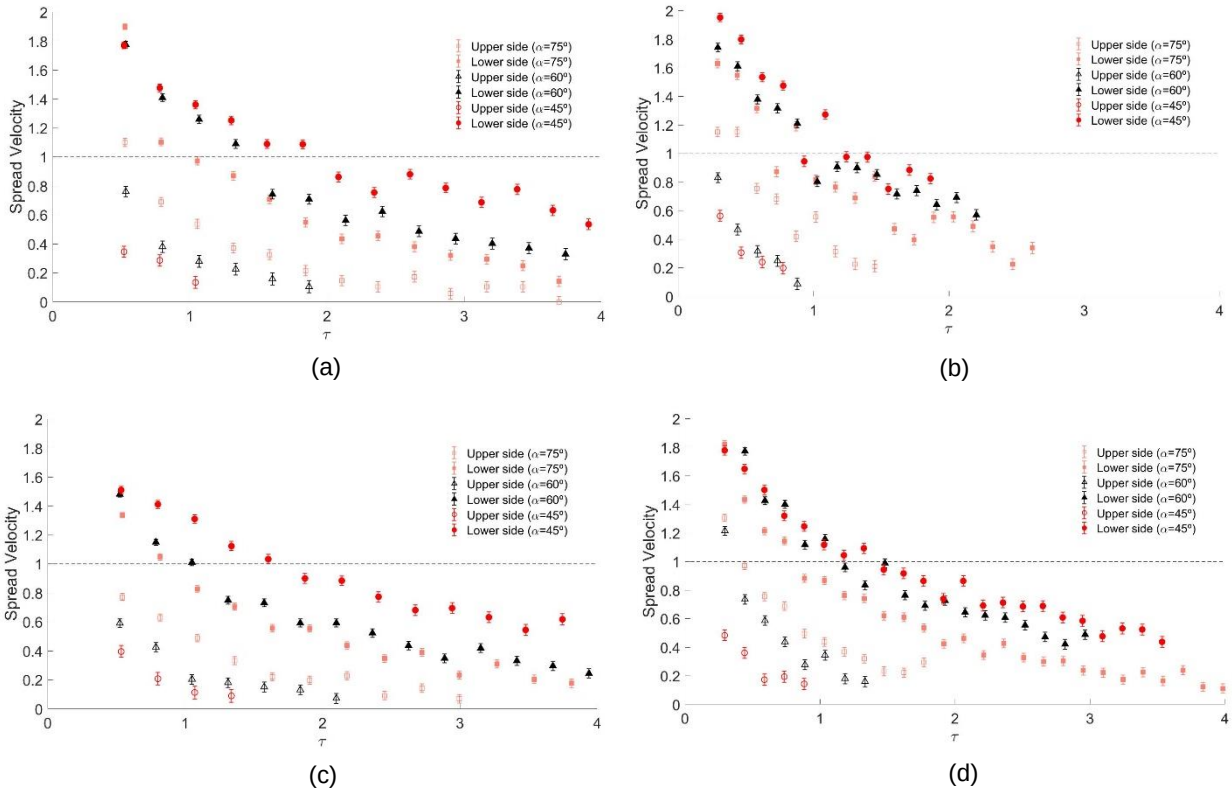

Figure 6. Spread Velocity as function of non-dimensional time; (a) 100% Jet-Fuel (We=1500), (b) 100% Jet-Fuel (We=480), (c) 75% Jet-Fuel – 25%HVO (We=1600), (d) 75% Jet-Fuel – 25% HVO (We=480).

The graphics above presented show that dimensionless velocities decrease with an increase of dimensionless time, which is consistent with the literature. At the initial stage, the spreading has a higher velocity and then stars to reduce until stabilizing. For H_2O and 50% JF – 50%HVO, the same results were observed.

Conclusions

The present work focuses on an experimental study of a single droplet impinging onto a dry, sloped surface. The purpose of this work was studying the influence on the droplet deformation after impact for a conventional Jet-Fuel (Jet A-1) and a Biofuel (HVO). This theme has a huge relevance on the modern days due to new environmental policies that promote the reduction of greenhouse gas emissions, pollutants, the need for fuel security and economic development. Therefore, it was concluded that not only the physical properties of fluids influence the phenomena observed but also the incident angle and the Weber number. For a We constant, splashing decreases with the decrease of the incident angle. However, when the We decreases, the splash is suppressed and the development of the lamella in the transverse and longitudinal direction is different. The dynamic behavior of the spreading was studied, and the spread velocity and spread factor were analyzed for different We and incident angles. The different component of gravity influences the expansion film that remains on the surface, which influences the spread factor. Thus, in the initial stages, the inertial forces prevail and then the effect of gravity has a significant role. It was noticed that an increase in We generates a higher spread factor for similar incident angles. Regarding the spread velocity,

the difference between the length for the upper and lower sides increases with the decrease of the incident angle. The morphology of liquid film on the lower side shows a larger spreading velocity.

Acknowledgements
The present work was performed for the interinstitutional project "BISI – Biofuel Spray Impact in Aero-Engines" under the scope of Laboratório Associado em Energia, Transportes e Aeronáutica (LAETA) – activities and it was supported by Fundação para a Ciência e Tecnologia (FCT) through the project UID/EMS/50022/2019.

Nomenclature

D_0	Droplet Diameter [mm]
HVO	Hydroprocessed Vegetable Oil
JF	Jet-Fuel
t	Time After Impact [ms]
u	Impact Velocity [ms^{-1}]
u_n	Normal Velocity Component [ms^{-1}]
u_t	Tangential Velocity Component [ms^{-1}]
We	Weber Number
α	Incident Angle [º]
ρ	Density [kg m^{-3}]
σ	Surface Tension [mN m^{-1}]
μ	Viscosity [mPa.s]
τ	Dimensionless Time
θ_a	Advancing Contact Angle [º]
θ_r	Receding Contact Angle [º]
θ_{static}	Static Contact Angle [º]

References

[1] Yarin, A. L., 2006, Annual Review of Fluid Mechanics, *38(1)*, pp. 159–192.
[2] Brown, R. A.,Orr, F. M. and. Scriven, L. E, 1980, Journal of Colloid and Interface Science*,73(1)*, pp. 76-87.
[3] Elsherbini, A. I., and Jacobi, A.M., 2004, Journal of Colloid and Interface Science.
[4] Rein, M., 1993, Fluid Dynamics Research, *12*, pp.61-93.
[5] Yao, S. C. and Cai, K. Y., 1988, Experimental Thermal and Fluid Science*, 1*, pp 363-371.
[6] Chen, R. H. and H. W. Wang*,* 2005, Experiments in Fluids*, 39*, pp.754-760.
[7] Bird, J. C., Tsai, S. S. H., and. Stone, H. A*,* 2009, New Journal of Physics, *11*.
[8] Jayaratne, O. W., and Mason, B. J.~, 1964, Proceedings of the Royal Society A: Mathematical, Physical and Engineering Sciences, *280*, pp. 545-565.
[9] Liu, J., Vu, H., Yoon, S., Jepsen, R. and Aguilar, G., 2010, Atomization and Sprays, *20*, pp. 297-310.
[10] Yeong, Y., Burton, J. and Loth, E., 2014, Langmuir.
[11] Liang, G., Guo, Y., Yang, Y., Zhen, N., and Shen, S., 2013, Langmuir, 30, pp. 12027-12038.
[12] Hao, J., Lu, J., Lee, L., Wu, Z., Hu, G., Floryan, J., 2019, Physical Review Letters*, 122,* pp. 54501.
[13] Zen, T., Chou, F., and Ma, J., 2010, International Communications in Heat and Mass Transfer, *37*, pp. 1025-1030.
[14] Bikerman, J., 1950, Journal of Colloid Science*, 5*, pp. 349-359.
[15] Liang, G., Guo, G., Shen, Y. and Yu, H., 2014, Acta Mechanica*.*
[16] Shen, C., Yu, C. and Chen, Y., 2015, Theoretical and Computational Fluid Dynamics, *30*, pp. 237-252.
[17] Šikalo, Š., Tropea C., and Ganic, E. N., 2015, Journal of Colloidal and Interface Science, *286*, pp. 661-669.
[18] Kang and Lee, 2000, Experiments in Fluids, *29*, pp. 380-387.
[19] Basit, A., KuShaari, K., Trinh, T., and Azeem, B.*,* 2014, International Journal of Chemical Engineering and Applications, *5*, pp. 95-99.
[20] Cui, J., Chen, X., Wang, F., Gong, X. and Yu, Z., 2009, Asia-Pacific Journal of Chemical Engineering.
[21] Roisman, I. V., Rioboo, R., and Tropea C., 2002, Proceedings of the Royal Society A: Mathematical, Physical and Engineering Sciencis, *458*, pp. 1411-1430.
[22] Liang, G., Guo, Y., Yang, Y., Zhen, N. and Shen, S., 2013, Acta Mechanica.
[23] D. Ribeiro, 2018, Experimental Study of a Single Droplet Impinging upon Liquid Films: Jet Fuel and Biofuel Mixtures